JAST, Vol. 12, No. 1, pp. 53- 63

JAST Journal of Aerospace Science and Technology

Nonlinear Vibration Analysis of Piezoelectric Functionally Graded Porous Timoshenko Beams

M. Zia[1], A. Nouri[2] and E. Hosseinian[3]*

1. Department of Mechanical Engineering, Faculty of Engineering, Imam Khomeini International University, Qazvin, Iran

2, 3.Department of Aerospace Engineering, Shahid Sattari Aeronautical University of Science and Technology

*Postal Code: 13846673411 ,Tehran, IRAN

ehosseinian@alum.sharif.edu

In this paper, nonlinear vibration analysis of functionally graded piezoelectric (FGP) beam with porous materials is investigated based on the Timoshenko beam theory. Material properties of FG porous beam are described according to the rule of mixture which is modified to approximate material properties with porosity phases. Ritz method is used to obtain the governing equation which is then solved by a direct iterative method to determine the nonlinear vibration frequencies of FGP porous beam subjected to different boundary conditions.The effects of external electric voltage, material distribution profile, porosity volume fraction, slenderness ratios and boundary conditions on the nonlinear vibration characteristics of the FGP porous beam are discussed in detail. The results indicate that piezoelectric layers have a significant effect on the nonlinear frequencies. Also, it is found that porosity has a considerable influence on the nonlinear frequency, especially when the electric voltage is applied.

Keywords: Nonlinear vibration, Porous material, Functionally graded material beam,Piezoelectric layers

Introduction

Functionally graded materials (FGMs), are a novel generation of composites of microscopic heterogeneity proposed in the early 1980s [1].These materials are supplied by controlling the volume fractions, microstructure, porosity, etc. of the material constituents during manufacturing, resulting in spatial gradient of macroscopic material properties of mechanical strength and thermal conductivity. As a result, FGMs possess various advantages over the conventional composite laminates, such as smaller thermal stresses, stress concentrations or intensity factors, attenuation of stress waves, and so on. [2].Due to the high mechanical and thermal properties of the ceramic-metal materials, FGMs have excellent resistance to high temperature and thermal impact [3]. Therefore, functionally graded materials have many applications in various branches of industry such as power, engineering, automotive and electronics industries [4].

With a browse of the previous studies, it is found that there are many investigations on vibration analysis of FGM beams. Kitipornchai et al. [5] analyzed nonlinear vibration of FG Timoshenko beam with an edge crack. They used Ritz method to derive the governing eigenvalue equation. Ke et al. [6] investigated the nonlinear free vibration of functionally graded nanocomposite beams reinforced by single-walled carbon nanotubes supported with different

boundary conditions.Longitudinal free vibration analysis of axially functionally graded microbars was conducted by Akgöz and Civalek [7]. They utilized Rayleigh-Ritz method to obtain an approximate solution for the beam with a clamped-clamped and clamped-free boundary conditions. Pradhan and Chakraverty [8] presented fundamental frequencies of FGM beams with different boundary conditions. Ansari et al. [9] investigated size-dependent vibration of functionally graded curved microbeams based on the modified strain gradient elasticity theory. Mashat et al. [10] used the Carrera Unified Formulation to carry out free-vibrational analyses of functionally graded structures. Hadji et al. [11] developed higher order shear deformation beam theory to perform static and free vibration analysis of functionally graded beams. Moreover, Sofiyev [12] studied vibration and stability of functionally graded conical shells under a compressive axial load within the framework of shear deformation beam theoryand using Galerkin's method.Chen et al. [13] studied thermo-elastic vibration of FGM beams with general boundary conditions based on a higher-order shear deformation beam theory. The size-dependent vibration behavior of the nano-beam made of functionally graded materials is also studied by Zhang et al. [14] based on the non-local theory and the material and dimensions of the beams. In all of these studies the effect of porosity was not considered.

Besides, due to porosity occurring inside FGMs during fabrication, FGMs can be modeled as a porous material with nonhomogeneous distribution of porosity. It is therefore necessary to consider the vibration behavior of beams having porosities in this study. Recently, researchers have investigated the vibration behavior of porous FGM beams. For example, the linear and nonlinear vibration analysis of FGM beam with porosities was done by Wattanasakulpong et al. [15]. They used differential transformation method to obtain linear and nonlinear vibration responses of porous FGM beams with different kinds of elastic supports. Ebrahimi and Zia [16] studied the large-amplitude nonlinear vibration of functionally graded (FG) Timoshenko beams made of porous material. They employed both Galerkin's method and the method of multiple scales to solve the governing equations. Chen et al. [17] studied the free and forced vibration characteristics of functionally graded porous beams with nonlinear distribution of elastic module and mass density along the thickness direction of the beam. They considered symmetric and asymmetric porosity distributions in their porous FGM beam.Shafiei et al. [18] analyzed size dependent nonlinear vibration behavior of imperfect uniform and non-uniform functionally graded micro beams within the framework of modified couple stress and Euler-Bernoulli theories. Ebrahimi et al. [19] conducted the thermo-mechanical vibration analysis of functionally graded beams made of a porous material subjected to various thermal loadings using the differential transformation method. Additionally, Gui-Lin et al. [20] investigated the vibration behaviors of porous nanotubes. They used the Navier solution method in order to solve the governing equations.

Because of their efficiency in converting electrical energy into mechanical energy, piezoelectric materials have found numerous applications in structural dynamics. Their main applications are in sensors and electromechanical actuators, as resonators in electronic equipment, also they have acoustic applications, as ultrasound transducers, naval hydrophones, and sonars. In addition, recently, the FGM concept has been applied to the piezoelectric structures such as bimorph actuators [21]. Yang and Zhifei [22] studied the free vibration of an FGP beam using state-space based differential quadrature method (SSDQM). Armin et al. [23] identified the static and dynamic characteristics of an FGP beam under thermal, electrical and mechanical loading using the finite element analysis. Doroushi et al. [24] presented the free and forced vibration characteristics of an FGPMbeam under thermo-electro-mechanical loads based on the higher-order shear deformation beamtheory. Ke et al. [25] investigated thermoelectric-mechanical vibration of the piezoelectric nanobeams using the nonlocal theory and Timoshenko beam theory.Electro-thermo-mechanical vibrational behavior of FGP plates with porosities is explored via a refined four-variable plate theory by Barati and Zenkour [26]. Furthermore, Ebrahimi and Salari [27] extracted the thermo-electro-mechanical vibrations of FGP Timoshenko nanobeam under thermal and electrical loading.Ebrahimi and Barati [28] conducted the nonlocal free vibration analysis of curved FGP nanobeams based on the Euler–Bernoulli beam model by using a Navier-type solution method.The steady-state analytical solutions for the coupled thermo-electro-elastic

forced vibrations of piezoelectric laminated beams are presented by Zhao et al. [29].

To the best knowledge of the authors, no research effort has been devoted so far to find theeffect of porosity on the nonlinear vibrational behavior of an FG Timoshenko beam with piezoelectric layers. Motivated by these considerations, in this investigation, the nonlinear vibration of piezoelectric FG porous beam is studied within the framework of Timoshenko beam theory and von Kármán geometric nonlinearity. The governing eigenvalue equation is derived by using Ritz method and a direct iterative method is used to obtain the nonlinear vibration frequencies of a piezoelectric FG porous beam subjected to three different boundary conditions, including hinged-hinged (H-H), clamped-clamped (C-C) and clamped-hinged (C-H). The influences of external electric voltage material distribution profile, porosity volume fraction, slenderness ratios and boundary conditions on the vibration behavior of the piezoelectric FG porous beam are discussed in detail. In order to validate the present study, the results of this paper are compared with the available results from the existing literature.

Piezoelectric Functionally Graded Porous Beam

An FG porous beam mounted with two piezoelectric layers on the top and bottom surfaces is shown in Fig. 1, with length L, and total thickness $h+2h_a$, where h is the thickness of the FG porous beam and $h_a$is the thickness of the piezoelectric layer. In this investigation, it is considered that the FG beam is comprised of ceramic and metal, and the effective material properties of the FG beams such as Young's modulus E, Poisson's ratio ν, shear modulus G and material density (ρ) vary constantly across the thickness direction based on the modified power-law model. Consider an imperfect FGM with a porosity volume fraction, α $(\alpha \ll 1)$, distributed evenly across the metal and ceramic, the modified rule of mixture is expressed by [15]:

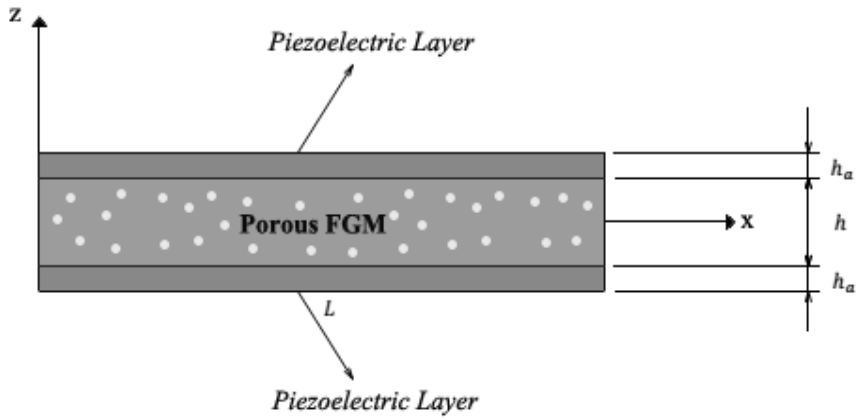

Figure 1. Functionally graded porous beam with piezoelectric layers

$$P = P_m\left(V_m - \frac{\alpha}{2}\right) + P_c\left(V_c - \frac{\alpha}{2}\right) \quad (1)$$

Now, the total volume fraction of the metal and ceramic is: $V_m + V_c = 1$, and the ceramic volume *fractions is stated as [15]:*

$$V_c = \left(\frac{z}{h} + \frac{1}{2}\right)^n \quad (2)$$

Therefore, all material properties of the imperfect FGM can be expressed as [15]:

$$P = (P_c - P_m)\left(\frac{z}{h} + \frac{1}{2}\right)^n + P_m - (P_m + P_c)\frac{\alpha}{2} \quad (3)$$

Where the positive real number n ($0 \le n < \infty$) is the power law or volume fraction index, and z is the distance from the mid-plane of the FG beam. The Young's modulus (E) and material density (ρ) equations of the imperfect FGM beam can be written as [15]:

$$E(z) = (E_c - E_m)\left(\frac{z}{h} + \frac{1}{2}\right)^n + E_m - (E_m + E_c)\frac{\alpha}{2} \quad (4)$$

$$\rho(z) = (\rho_c - \rho_m)\left(\frac{z}{h} + \frac{1}{2}\right)^n + \rho_m - (\rho_m + \rho_c)\frac{\alpha}{2} \quad (5)$$

Theoretical formulation

This investigation is based on the Timoshenko beam theory with the following displacement field [32]:

$$\widetilde{U}(x.z.t) = U(x.t) + z\psi(x.t), \quad \widetilde{W}(x.z.t) = W(x.t) \tag{6}$$

Where $U(x,t)$and $W(x,t)$are the axial and the transverse displacement in the midplane, ψ is the rotation of beam cross-section and t is time. The Von-Kármán type nonlinear strain-displacement relationships are given by:

$$\varepsilon_x = \frac{\partial U}{\partial x} + z\frac{\partial \psi}{\partial x} + \frac{1}{2}\left(\frac{\partial W}{\partial x}\right)^2, \ \gamma_{xz} = \frac{\partial W}{\partial x} + \psi \tag{7}$$

Where ε_x and γ_{xz} are the normal and shear strains, respectively.

For the piezoelectric layer electric field component, E_z can be written as (Shen [30]):

$$E_z = \frac{V_0}{h_a} \tag{8}$$

Where $V_0$is the applied voltage across the thickness.

The constitutive relations for the functionally graded porous beam are given as follows (Ke et al. [25]):

$$\sigma_{xx} = Q_{11}(z)\left[\frac{\partial U}{\partial x} + z\frac{\partial \psi}{\partial x} + \frac{1}{2}\left(\frac{\partial W}{\partial x}\right)^2\right] \tag{9}$$

$$, \quad \sigma_{xz} = Q_{55}(z)\left(\frac{\partial W}{\partial x} + \psi\right)$$

$$Q_{11}(z) = \frac{E(z)}{1-\upsilon(z)^2} \quad , \quad Q_{55}(z) = \frac{E(z)}{2(1+\upsilon(z))}$$

And for the piezoelectric layers:

$$\sigma_{xx}^a = c_{11}\varepsilon_{xx} - e_{31}E_z \ , \ D_z = e_{31}\varepsilon_{xx} + \epsilon_{33}E_z$$

$$\sigma_{xz}^a = \frac{c_{11}}{2(1+\upsilon_a)}\gamma_{xz} \ , \quad Q_{55a} = \frac{k_s\, c_{11}}{2(1+\upsilon_a)} \tag{10}$$

Where$\sigma_{xx}$and σ_{xz} are the axial and shear stresses through the FG porous beam and σ_{xx}^a and σ_{xz}^a are the axial and shear stresses through the piezoelectric layers.Q_{11}andQ_{55}arereduced elastic constants. Also, $\upsilon(z)$ and $\upsilon_a$are Poisson's ratios for FG porous beam and piezoelectric layers, respectively. Here, c_{11},D_z,e_{31}, and ϵ_{33} are the elastic constant, electric displacement, piezoelectric constant, and the dielectric permittivity coefficient for the piezoelectric layers, respectively.

For the FGP porous Timoshenko beam, the kinetic energy T and potential energy V can be written as:

$$\begin{aligned} T = {} & \frac{1}{2}\int_0^l \int_{-\frac{h}{2}}^{\frac{h}{2}} \rho(z)\left[\left(\frac{\partial U}{\partial t} + z\frac{\partial \psi}{\partial t}\right)^2 + \right. \\ & + \frac{1}{2}\int_0^l \int_{\frac{h}{2}}^{\frac{h}{2}+h_a} \rho_a\left[\left(\frac{\partial U}{\partial t} + z\frac{\partial \psi}{\partial t}\right)^2 + \left(\frac{\partial W}{\partial t}\right)^2\right] dzdx \\ & \left.\left(\frac{\partial W}{\partial t}\right)^2\right] dzdx + \frac{1}{2}\int_0^l \int_{-\frac{h}{2}-h_a}^{-\frac{h}{2}} \rho_a\left[\left(\frac{\partial U}{\partial t} + z\frac{\partial \psi}{\partial t}\right)^2 + \right. \\ & \left.\left(\frac{\partial W}{\partial t}\right)^2\right] dzdx \end{aligned} \tag{11}$$

$$\begin{aligned} V = {} & \frac{1}{2}\int_0^l \int_{-\frac{h}{2}}^{\frac{h}{2}} \left\{Q_{11}(z)\left[\left(\frac{\partial U}{\partial x} + z\frac{\partial \psi}{\partial x}\right) + \right.\right. \\ & \left.\left. \frac{1}{2}\left(\frac{\partial W}{\partial x}\right)^2\right]^2 + Q_{55}(z)\left(\frac{\partial W}{\partial x} + \psi\right)^2\right\} dzdx \\ & + \frac{1}{2}\int_0^l \int_{\frac{h}{2}}^{\frac{h}{2}+h_a} \left\{\left[c_{11}\left(\left(\frac{\partial U}{\partial x} + z\frac{\partial \psi}{\partial x}\right) + \frac{1}{2}\left(\frac{\partial W}{\partial x}\right)^2\right)^2 - \right.\right. \\ & \left. e_{31}E_z\left[\left(\frac{\partial U}{\partial x} + z\frac{\partial \psi}{\partial x}\right) + \frac{1}{2}\left(\frac{\partial W}{\partial x}\right)^2\right]\right] + \\ & Q_{55a}\left(\frac{\partial W}{\partial x} + \psi\right)^2 - \\ & \left. D_zE_z\right\} dzdx + \frac{1}{2}\int_0^l \int_{-\frac{h}{2}-h_a}^{-\frac{h}{2}} \left\{\left[c_{11}\left(\left(\frac{\partial U}{\partial x} + z\frac{\partial \psi}{\partial x}\right) + \right.\right.\right. \\ & \left.\left. \frac{1}{2}\left(\frac{\partial W}{\partial x}\right)^2\right)^2 - e_{31}E_z\left[\left(\frac{\partial U}{\partial x} + z\frac{\partial \psi}{\partial x}\right) + \right.\right. \\ & \left.\left.\left. \frac{1}{2}\left(\frac{\partial W}{\partial x}\right)^2\right]\right] + Q_{55a}\left(\frac{\partial W}{\partial x} + \psi\right)^2 - D_zE_z\right\} dzdx \end{aligned} \tag{12}$$

Also, the work done by the external force can be expressed as:

$$W_{ex} = \int_0^l \quad f_p\left(\frac{\partial W}{\partial x}\right)^2 dx \tag{13}$$

Where $f_p$is the normal force induced by the external electric voltage V_0, and can be written as:

$$f_p = \int_{\frac{h}{2}}^{\frac{h}{2}+h_a} e_{31}E_z dz + \int_{-\frac{h}{2}-h_a}^{-\frac{h}{2}} e_{31}E_z dz \tag{14}$$

The stiffness components and inertia related terms can be stated as:

$$(A_{11}, B_{11}, D_{11}) = \int_{-\frac{h}{2}}^{\frac{h}{2}} \frac{E(z)}{1-\upsilon(z)^2}(1, z, z^2)dz$$

$$A_{55} = \int_{-\frac{h}{2}}^{\frac{h}{2}} \frac{k_s E(z)}{2(1+\upsilon)}dz$$

$$(A_{11a}, B_{11a}, D_{11a}) = \int_{\frac{h}{2}}^{\frac{h}{2}+h_a} c_{11}\,(1, z, z^2)dz + \int_{-\frac{h}{2}-h_a}^{-\frac{h}{2}} c_{11}\,(1, z, z^2)dz$$

$$A_{55a} = \int_{\frac{h}{2}}^{\frac{h}{2}+h_a} \frac{k_s\, c_{11}}{2(1+\upsilon_a)}dz + \int_{-\frac{h}{2}-h_a}^{-\frac{h}{2}} \frac{k_s\, c_{11}}{2(1+\upsilon_a)}dz \quad (15)$$

$$(I_1, I_2, I_3) = \int_{-h/2}^{h/2} \rho(z)(1, z, z^2)dz$$

$$(I_{1a}, I_{2a}, I_{3a}) = \int_{\frac{h}{2}}^{\frac{h}{2}+h_a} \rho_a(1, z, z^2)dz + \int_{-\frac{h}{2}-h_a}^{-\frac{h}{2}} \rho_a(1, z, z^2)dz$$

Where k_s= 5/6 is the shear correction factor and also $\rho(z)$ andρ_a are the mass densities of FGM and piezoelectric layer, respectively.

For a beam that is undergoing harmonic motion, the maximum kinetic energy of beam $T_{\max}$ can be stated as:

$$T_{\max} = \frac{\Omega^2}{2}\left\{\begin{array}{l}\int_0^l (I_1 U^2 + 2I_2 U\psi + I_3\psi^2 + I_1 W^2)dx + \\ \int_0^l (I_{1a} U^2 + 2I_{2a} U\psi + I_{3a}\psi^2 + I_{1a} W^2)dx\end{array}\right\} \quad (16)$$

Where Ω is the nonlinear frequency of the FGP beam. And also the maximum potential energy $V_{\max}$ of the FGP beam can be stated as [6]:

$$V_{\max} = V_{\text{linear}} + V_{\text{nonlinear}} \quad (17)$$

Where V_{linear} and $V_{\text{nonlinear}}$ are linear and nonlinear potential energies according to strain-displacement relationships and can be written as:

$$V_{\text{linear}} = \frac{1}{2}\left\{\begin{array}{l}\int_0^l \left(\begin{array}{c} A_{11}\left(\frac{\partial U}{\partial x}\right)^2 + 2B_{11}\frac{\partial U}{\partial x}\frac{\partial \psi}{\partial x} + D_{11}\left(\frac{\partial \psi}{\partial x}\right)^2 \\ +A_{55}\left(\frac{\partial W}{\partial x}+\psi\right)^2\end{array}\right)dx + \\ \int_0^l \left(\begin{array}{c} A_{11a}\left(\frac{\partial U}{\partial x}\right)^2 + 2B_{11a}\frac{\partial U}{\partial x}\frac{\partial \psi}{\partial x} + D_{11a}\left(\frac{\partial \psi}{\partial x}\right)^2 \\ +A_{55a}\left(\frac{\partial W}{\partial x}+\psi\right)^2\end{array}\right)dx + \\ \int_0^l \left(-4e_{31}V_0\left(\frac{\partial U}{\partial x}+\frac{1}{2}\left(\frac{\partial W}{\partial x}\right)^2\right)\right)dx + \int_0^l (-2V_0\epsilon_{33}E_z)dx\end{array}\right\} \quad (18)$$

$$V_{\text{nonlinear}} = \frac{1}{2}\left\{\begin{array}{l}\int_0^l \left(\begin{array}{c} A_{11}\frac{\partial \psi}{\partial x}\left(\frac{\partial W}{\partial x}\right)^2 + B_{11}\frac{\partial U}{\partial x}\left(\frac{\partial W}{\partial x}\right)^2 \\ +\frac{1}{4}A_{11}\left(\frac{\partial W}{\partial x}\right)^4\end{array}\right)dx \\ +\int_0^l \left(\begin{array}{c} A_{11a}\frac{\partial \psi}{\partial x}\left(\frac{\partial W}{\partial x}\right)^2 + B_{11a}\frac{\partial U}{\partial x}\left(\frac{\partial W}{\partial x}\right)^2 \\ +\frac{1}{4}A_{11a}\left(\frac{\partial W}{\partial x}\right)^4\end{array}\right)dx\end{array}\right\} \quad (19)$$

And external work can be stated as:

$$W_{ex} = \int_0^l \quad 2e_{31}V_0\left(\frac{\partial W}{\partial x}\right)^2 dx \quad (20)$$

By defining the following normalized variables:

$$\hat{x} = \frac{x}{l},\ (\hat{U}, \hat{W}) = \left(\frac{U}{h}, \frac{W}{h}\right),$$
$$(\hat{I}_1, \hat{I}_2, \hat{I}_3, \hat{I}_{1a}, \hat{I}_{2a}, \hat{I}_{3a}) = \left(\frac{I_1}{I_{10}}, \frac{I_2}{I_{10}h}, \frac{I_3}{I_{10}h^2}, \frac{I_{1a}}{I_{10}}, \frac{I_{2a}}{I_{10}h}, \frac{I_{3a}}{I_{10}h^2}\right)$$
$$(\hat{A}_{11}, \hat{A}_{55}, \hat{B}_{11}, \hat{D}_{11}, \hat{A}_{11a}, \hat{A}_{55a}, \hat{B}_{11a}, \hat{D}_{11a}) = \left(\begin{array}{l}\frac{A_{11}}{A_{110}}, \frac{A_{55}}{A_{110}}, \frac{B_{11}}{A_{110}h}, \frac{D_{11}}{A_{110}h^2} \\ , \frac{A_{11a}}{A_{110}}, \frac{A_{55a}}{A_{110}}, \frac{B_{11a}}{A_{110}h}, \frac{D_{11a}}{A_{110}h^2}\end{array}\right) \quad (21)$$
$$\eta = \frac{l}{h},\ \hat{\phi} = \frac{e_{31}V_0}{A_{110}},\ \hat{\varphi} = \frac{\epsilon_{33}V_0E_z}{A_{110}},$$
$$\omega = \Omega l\sqrt{\frac{I_{10}}{A_{110}}}$$

Where A_{110} and I_{10} are the values of A_{11} and I_1 of a homogeneous beam (n→ ∞), the normalized form of Eqs. (16-20) can be stated as:

Where

$$\bar{T}_{\max} = \frac{T_{\max}}{\mu}, \bar{V}_{\text{linear}} = \frac{V_{\text{linear}}}{\mu}, \bar{V}_{\text{nonlinear}} \quad (22)$$

$$= \frac{V_{\text{nonlinear}}}{\mu}, \bar{W}_{ex} = \frac{W_{ex}}{\mu}, \mu = \frac{A_{110}h^2}{l}$$

$$\bar{V}_{\text{linear}} = \frac{1}{2}\left\{\begin{array}{c} \int_0^1 \left(\begin{array}{c} \hat{A}_{11}\left(\frac{\partial \hat{U}}{\partial \hat{x}}\right)^2 + 2\hat{B}_{11}\frac{\partial \hat{U}}{\partial \hat{x}}\frac{\partial \psi}{\partial \hat{x}} + \\ \hat{D}_{11}\left(\frac{\partial \psi}{\partial \hat{x}}\right)^2 + \hat{A}_{55}\left(\frac{\partial \hat{W}}{\partial \hat{x}} + \eta\hat{\psi}\right)^2 \end{array}\right) d\hat{x} + \\ \int_0^1 \left(\begin{array}{c} \hat{A}_{11a}\left(\frac{\partial \hat{U}}{\partial \hat{x}}\right)^2 + 2\hat{B}_{11a}\frac{\partial \hat{U}}{\partial \hat{x}}\frac{\partial \psi}{\partial \hat{x}} \\ +\hat{D}_{11a}\left(\frac{\partial \psi}{\partial \hat{x}}\right)^2 + \hat{A}_{55a}\left(\frac{\partial \hat{W}}{\partial \hat{x}} + \eta\psi\right)^2 \end{array}\right) d\hat{x} + \\ \int_0^1 -4\hat{\phi}\left(\eta\frac{\partial \hat{U}}{\partial \hat{x}} + \frac{1}{2}\left(\frac{\partial \hat{W}}{\partial \hat{x}}\right)^2\right) d\hat{x} + \int_0^1 -2\eta^2\hat{\varphi} d\hat{x} \end{array}\right\} \tag{23}$$

$$\bar{V}_{\text{nonlinear}} = \frac{1}{2}\left\{\begin{array}{c} \int_0^1 \left(\begin{array}{c} \frac{\hat{A}_{11}}{\eta}\frac{\partial \psi}{\partial \hat{x}}\left(\frac{\partial \hat{W}}{\partial \hat{x}}\right)^2 \\ +\frac{\hat{B}_{11}}{\eta}\frac{\partial \hat{U}}{\partial \hat{x}}\left(\frac{\partial \hat{W}}{\partial \hat{x}}\right)^2 \\ +\frac{\hat{A}_{11}}{4\eta^2}\left(\frac{\partial \hat{W}}{\partial \hat{x}}\right)^4 \end{array}\right) d\hat{x} \\ + \int_0^1 \left(\begin{array}{c} \frac{\hat{A}_{11a}}{\eta}\frac{\partial \psi}{\partial \hat{x}}\left(\frac{\partial \hat{W}}{\partial \hat{x}}\right)^2 \\ +\frac{\hat{B}_{11a}}{\eta}\frac{\partial \hat{U}}{\partial \hat{x}}\left(\frac{\partial \hat{W}}{\partial \hat{x}}\right)^2 \\ +\frac{\hat{A}_{11a}}{4\eta^2}\left(\frac{\partial \hat{W}}{\partial \hat{x}}\right)^4 \end{array}\right) d\hat{x} \end{array}\right\} \tag{25}$$

$$\bar{W}_{ex} = \int_0^1 2\hat{\phi}\left(\frac{\partial \hat{W}}{\partial \hat{x}}\right)^2 d\hat{x} \tag{26}$$

Where

$$\bar{T}_{\max} = \frac{T_{\max}}{\mu},\ \bar{V}_{\text{linear}} = \frac{V_{\text{linear}}}{\mu},$$

$$\bar{V}_{\text{nonlinear}} = \frac{V_{\text{nonlinear}}}{\mu},$$

$$\bar{W}_{ex} = \frac{W_{ex}}{\mu},\ \mu = \frac{A_{110}h^2}{l}$$

Therefore, the energy functional for the FGP beam can be stated as:

$$L = \bar{V}_{\text{linear}} + \bar{V}_{\text{nonlinear}} - \bar{T}_{\max} + \bar{W}_{ex} \tag{27}$$

Ritz method

In this investigation, Ritz method is used to obtain the governing eigenvalue equation for nonlinear vibration of FGP Timoshenko beams. Ritz trial displacement functions that satisfy the geometric boundary conditions of the beam can be written as:

$$\begin{aligned} \hat{U}(\hat{x}) &= \sum_{j=1}^{N} \lambda_{1j}\hat{x}^j(1-\hat{x})^{q_0} \\ \hat{W}(\hat{x}) &= \sum_{j=1}^{N} \lambda_{2j}\hat{x}^j(1-\hat{x})^{q_0} \\ \psi(\hat{x}) &= \textstyle\sum_{j=1}^{N} \lambda_{3j}\hat{x}^{(j+r_0)}(1-\hat{x})^{s_0} \end{aligned} \tag{28}$$

Where N is the number of polynomials involved in the trial functions, λ_{1j}, λ_{2j}, λ_{3j} are the unknown constant coefficients to be determined, and q_0, r_0, s_0 are trail function indices for different boundary conditions as stated in Table 1.

Table 1. Trial function indices for different boundary conditions

BCs	q_0	r_0	s_0
H–H	1	-1	0
C–H	1	0	0
C–C	1	0	1

Substituting the above trial functions into Eqs. (22–25); then applying Ritz method to minimize the total energy functional with respect to unknown coefficients:

$$\frac{\partial L}{\partial \lambda_{ij}} = 0\,, (i = 1,2,3; j = 1,2,\dots,N) \tag{29}$$

leads to nonlinear governing equation in matrix form:

$$([F] + [k_l] + [k_{nl}])[d] - \omega^2[M][d] = 0 \tag{30}$$

Where M is the mass matrix and k_l,k_{nl} are the linear and nonlinear stiffness matrices, respectively; the unknown vector is $d = \left\{\{\lambda_{1j}\}^T\{\lambda_{2j}\}^T\{\lambda_{3j}\}^T\right\}$ and F is the force matrix due to external electric voltage.

By neglecting nonlinear stiffness matrixk_{nl}, linear frequencies of the FGP beam can be obtained. Also, the direct iterative method is used to obtain nonlinear frequencies as stated by Ke et al. [6] before. In order to better describe the method used, the flowchart of solving method is illustrated in Fig. 2.

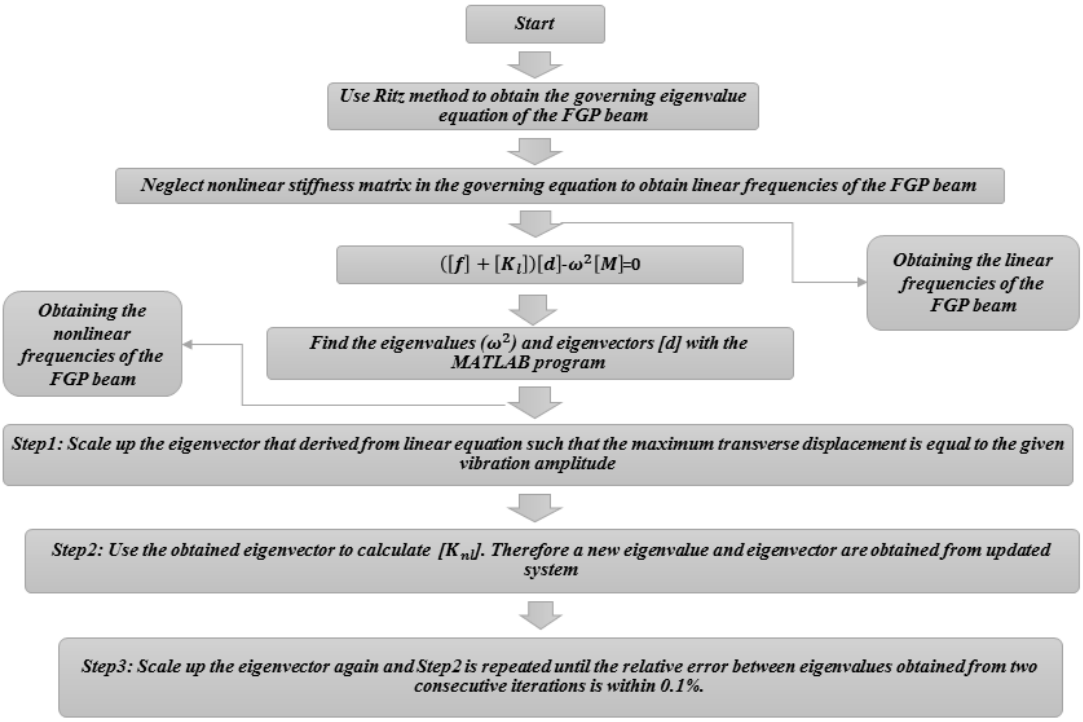

Figure 2. The flowchart of solving method

Numerical results

In this investigation, functionally graded material of the beam is composed of Alumina (Al_2O_3) and Aluminum (Al); the material properties of which are: E=380 GPa, ρ=3960 kg/m3, and υ=0.3 for Al_2O_3; and E=70 GPa, ρ=2702 kg/m3, and ν=0.3 for Al. Also, the piezoelectric layers are made of PZT-4 with the thickness of $h_a = 0.001m$, the material properties of which are: $c_{11} = 132$ Gpa, $e_{31} = -4.1$ C m^{-2} , $\epsilon_{33} = 7.124 \times 10^{-9}$ C $m^{-2}N^{-1}$, and $\rho_a = 7500$ kg/m3 (Ke et al. [25]). Before the vibration behaviors of the FGP porous Timoshenko beam are investigated, in order to ensure the accuracy of the present formulation, results obtained from the present study are compared with the other available results. The present results, linear fundamental frequency of intact FGM beams($\alpha = 0\,, h_a = 0$) are compared with those of Ke et al.[5] for different boundary conditions and slenderness ratios in Table 2. According to Table 2, the present results are in a good agreement with their analytical results. To further verify the present results, the nonlinear frequency ratio of ω_{nl}/ω_l for intact FGM beams is compared to the results obtained by Kitipornchai et al. [5] for different boundary conditions and amplitudes. The contents of Table 3 indicate that the present results are in a good agreement with their results.

Table 2. Comparison of linear fundamental frequency of intact FGM beams ($\omega = \Omega l\sqrt{\frac{I_{10}}{A_{110}}}, \alpha = 0\,, h_a = 0$)

		H-H			C-C		
l/h	n	Present	[31]	Error%	Present	[31]	Error%
6	0.2 1 5	0.4598 0.4521 0.4598	0.4543 0.4472 0.4543	1.21 1.09 1.21	0.8600 0.8991 0.8600	0.8494 0.8887 0.8494	1.25 1.17 1.25
16	0.2 1 5	0.1800 0.1768 0.1800	0.1797 0.1764 0.1797	0.17 0.23 0.17	0.3693 0.3918 0.3693	0.3686 0.3910 0.3686	0.19 0.20 0.19

Table 3. Comparison of nonlinear frequency ratio ω_{nl}/ω_l for intact FGM beams ($\omega = \Omega l\sqrt{\frac{I_{10}}{A_{110}}}$,l/h=6,$\alpha = 0, h_a = 0$)

BCs	n	w_{max}= 0.2			w_{max} = 0.4		
		Present	[5]	Error %	Present	[5]	Error %
H-H	0. 2 1 5	1.0332 1.0629 1.0334	1.021 7 1.072 7 1.032 3	1.13 0.91 0.11	1.1179 1.2320 1.1967	1.112 4 1.231 7 1.201 3	0.49 0.02 0.38
C-H	0. 2 1 5	1.0331 1.0347 1.0332	1.028 6 1.032 6	0.44 0.20 0.11	1.1191 1.1300 1.1357	1.110 0 1.123 9	0.82 0.54 0.27

			1.0321			1.1326	
C-C	0.2 1 5	1.0193 1.0175 1.0193	1.0192 1.0174 1.0192	0.01 0.01 0.01	1.0746 1.0677 1.0746	1.0744 1.0676 1.0744	0.02 0.01 0.02

Now, the numerical results for the hinged-hinged (H-H), clamped-hinged (C-H) and clamped-clamped (C-C) piezoelectric functionally graded porous Timoshenko beams are presented. Table 4 presents the effect of applied voltage on ω_{nl} for intact FGP beams in different amplitudes and volume fraction indexes. The results indicate that ω_{nl} decreases in positive voltage while increases in negative voltage. These variations are more significant at higher values of volume fraction index. The maximum increase and decrease for ω_{nl} in comparison with zero voltages are 11.32% and 13.13% respectively, and they occur at n = 5 and w_{max}= 0.8. Table 5 tabulatesvariation of ω_{nl} for different porosity coefficients and voltages. It is found that by increasing the porosity coefficient, ω_{nl} decreases, especially at higher values of volume fraction index in the positive voltage. Also, the maximum decrease for ω_{nl} in comparison with intact beam is 54.54% and occurs at n = 10, α = 0.2 and V_0=0.05. In Figs. (3-5) the effect of porosity coefficient on ω_{nl} of C-C FGP porous beam versus volume fraction index (n) in different voltages is illustrated.

Table 4. Effect of applied voltage on nonlinear frequency ω_{nl} for intact FGP beams in different amplitudes (l/h=6, α=0 and C-C boundary condition)

V_0	n	w_{max}			
		0.2	0.4	0.6	0.8
+0.05	0.2	1.52	1.61	1.75	1.93
	1	1.21	1.30	1.43	1.60
	2	1.05	1.14	1.26	1.41
	5	0.92	0.99	1.10	1.23
0	0.2	1.65	1.73	1.86	2.03
	1	1.39	1.46	1.58	1.73
	2	1.26	1.33	1.44	1.57
	5	1.17	1.22	1.31	1.42
-0.05	0.2	1.77	1.84	1.97	2.12
	1	1.54	1.61	1.71	1.85
	2	1.44	1.50	1.59	1.71
	5	1.36	1.41	1.48	1.58

Table 5. Variation of nonlinear frequency ω_{nl} of FGP beams for different porosity coefficients (l/h=6, w_{max}=0.2 and C-C boundary condition)

α	V_0	n=0.2	n=0.5	n=1	n=2	n=5	n=10
0	+0.05v	1.52	1.37	1.21	1.05	0.92	0.84
	0v	1.65	1.52	1.39	1.26	1.17	1.11
	-0.05v	1.77	1.66	1.54	1.44	1.36	1.32
0.1	+0.05v	1.52	1.36	1.16	0.96	0.79	0.69
	0v	1.66	1.52	1.36	1.21	1.10	1.04
	-0.05v	1.79	1.67	1.54	1.41	1.33	1.28
0.2	+0.05v	1.53	1.34	1.10	0.82	0.54	0.38
	0v	1.68	1.52	1.33	1.13	0.98	0.91
	-0.05v	1.82	1.68	1.53	1.37	1.26	1.22

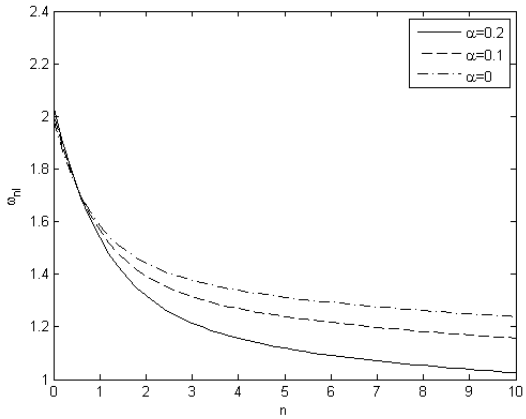

Figure 3. Variation of nonlinear frequency of C-C FGP porous beams versus volume fraction index for different porosity coefficients (l/h = 6, V_0= 0, w_{max}= 0.6)

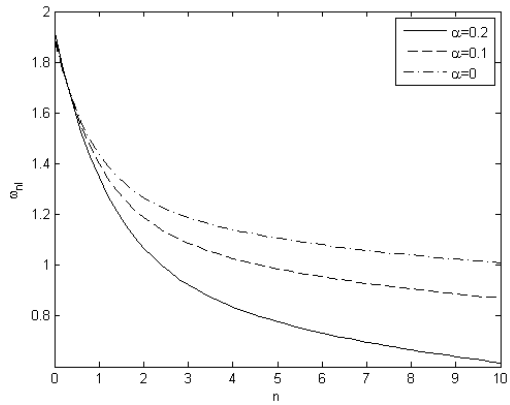

Figure 4. Variation of nonlinear frequency of C-C FGP porous beams versus volume fraction index for different porosity coefficients (l/h = 6, V_0= 0.05, w_{max}= 0.6)

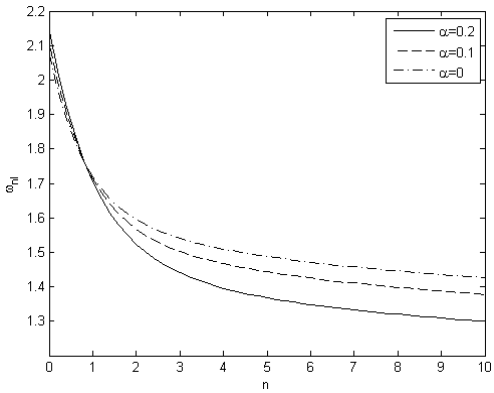

Figure 5. Variation of nonlinear frequency of C-C FGP porous beams versus volume fraction index for different porosity coefficients (l/h = 6, V_0= -0.05,w_{max}= 0.6)

Results indicate that with an increased porosity coefficient, ω_{nl} decreases and this phenomenon is more significant in a positive voltage. In Figs. (6-8) the effect of electric voltage on ω_{nl} of C-C FGP porous beam versus maximum amplitude w_{max} in different slender ratios is illustrated. As expected, the beam with a higher amplitude has a remarkably higher frequency, especially in the negative voltage and with a larger slender ratio.

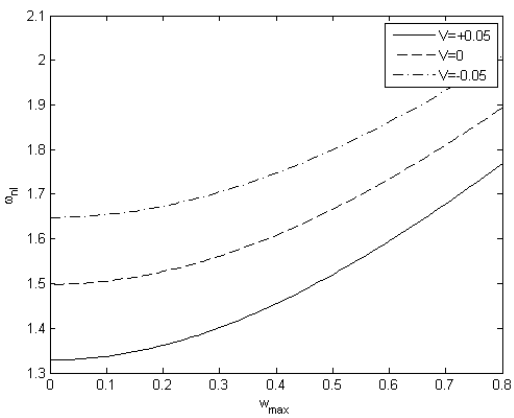

Figure 6. Variation of nonlinear frequency of FGP porous beams versus maximum amplitude for different voltages (l/h = 6, $\alpha = 0.1, n = 0.5$)

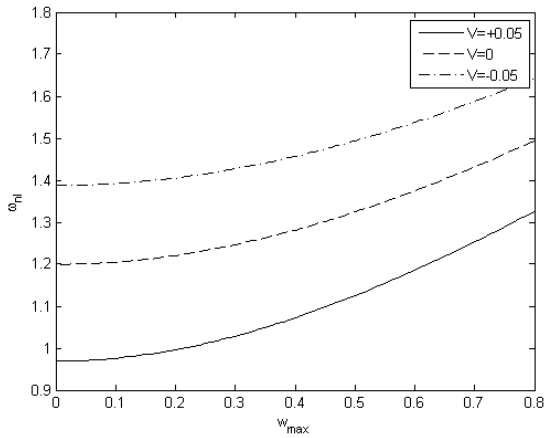

Figure 7. Variation of nonlinear frequency of FGP porous beams versus maximum amplitude for different voltages (l/h = 8,$\alpha = 0.1$, n= 0.5)

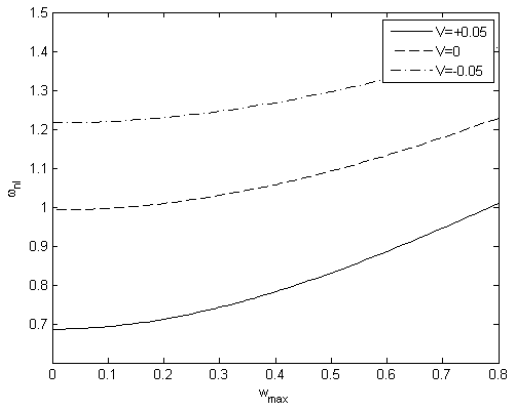

Figure 8. Variation of nonlinear frequency of FGP porous beams versus maximum amplitude for different voltages (l/h = 10,$\alpha = 0.1$, n= 0.5)

The effect of different boundary conditions on ω_{nl} versus volume fraction index (n) for different porosity coefficients is presented in Figs. (9-11). It is found that an increase in the volume fraction index has a significant effect on $\omega_{nl}$for higher porosity coefficients. The variation of ω_{nl} of FGP porous beam versus applied electric voltage for various boundary conditions is illustrated in Fig. 12. This figure shows that the effect of voltage is more significant for hinged-hinged boundary condition.

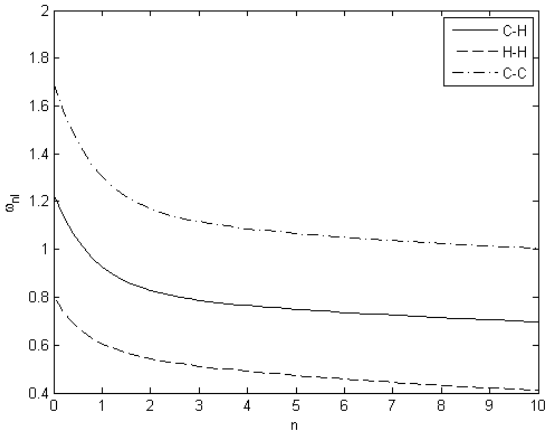

Figure 9. Variation of nonlinear frequency of FGP porous beams versus volume fraction index for different boundary conditions ($\alpha = 0$, l/h = 6, V_0= 0.02, w_{max}= 0.1)

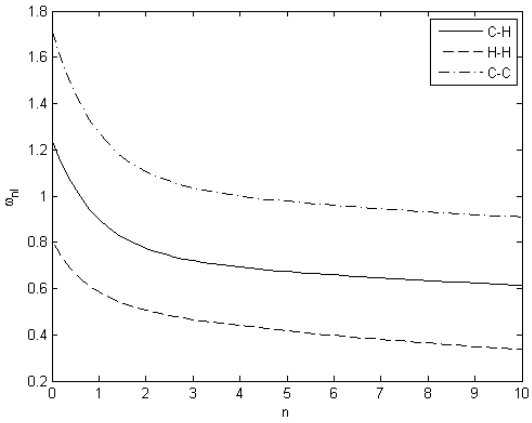

Figure 10. Variation of nonlinear frequency of FGP porous beams versus volume fraction index for different boundary conditions ($\alpha = 0.1$, l/h = 6, V_0= 0.02, w_{max}= 0.1)

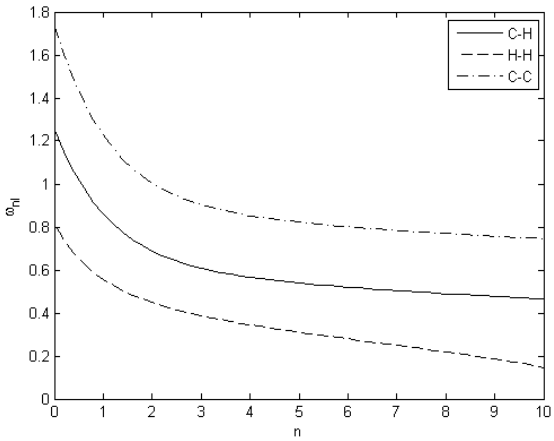

Figure 11. Variation of nonlinear frequency of FGP porous beams versus volume fraction index for different boundary conditions ($\alpha = 0.2$, l/h = 6, V_0= 0.02, w_{max}= 0.1)

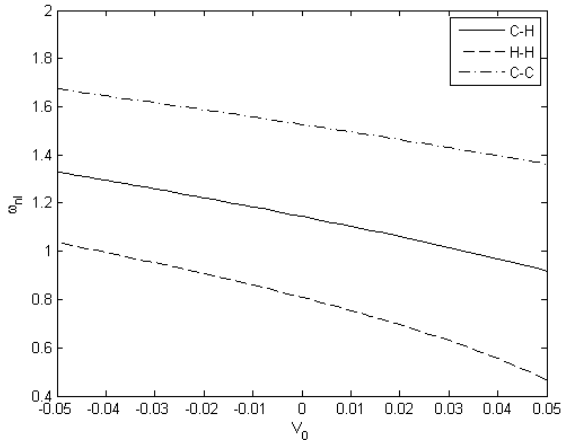

Figure 12. Variation of nonlinear frequency of FGP porous beams versus voltage for different boundary conditions (l/h = 6, $\alpha = 0.1, n$ = 0.5, w_{max}= 0.2)

Conclusions

In this paper, the nonlinear vibration analysis of functionally graded piezoelectric (FGP) beam with porous materials is conducted within the framework of Timoshenko beam theory and von Kármán geometric nonlinearity. The modified rule of mixture covering porosity phases is employed to describe and approximate material properties of the imperfect FGM beams. In this investigation, Ritz and direct iterative methods are used to obtain the nonlinear vibration frequencies of a piezoelectric FG porous beam subjected to three different boundary conditions of hinged-hinged (H-H), clamped-clamped (C-C) and clamped-hinged (C-H). The good agreement between the results of this article and those available in the literature verified the presented approach. The influences of several parameters such as external electric voltage, material distribution profile, porosity volume fraction, slenderness ratios and boundary conditions on the nonlinear vibration characteristics of the FGP porous beams are studied and discussed in detail. The numerical results indicate that porosity has a considerable effect on the vibrational behavior of the FGP beams and it is more significant when the electric voltage is applied. The maximum decrease for ω_{nl} is obtained as 54.54% in comparison with intact beam. Also, the effect of the applied voltage is more at higher amplitudes and the maximum increase and decrease for ω_{nl} in comparison with

zero voltages are obtained 11.32% and 13.13%, respectively, at n = 5 and w_{max}= 0.8.

References

[1] Koizumi M (1997) FGM activities in Japan. Composites Part B: Engineering 28 (1):1-4

[2] Ebrahimi F (2013) Analytical investigation on vibrations and dynamic response of functionally graded plate integrated with piezoelectric layers in thermal environment. Mechanics of Advanced Materials and Structures 20 (10):854-870

[3] El-wazery M, El-Desouky A (2015) A review on functionally graded ceramic-metal materials. J Mater Environ Sci 6 (5):1369-1376.

[4] Chmielewski M, Pietrzak K (2016) Metal-ceramic functionally graded materials–manufacturing, characterization, application. Bulletin of the Polish Academy of Sciences Technical Sciences 64 (1):151-160.

[5] Kitipornchai S, Ke L, Yang J, Xiang Y (2009) Nonlinear vibration of edge cracked functionally graded Timoshenko beams. Journal of sound and vibration 324 (3):962-982

[6] Ke L-L, Yang J, Kitipornchai S (2010) Nonlinear free vibration of functionally graded carbon nanotube-reinforced composite beams. Composite Structures 92 (3):676-683

[7] Akgöz B, Civalek Ö (2013) Longitudinal vibration analysis of strain gradient bars made of functionally graded materials (FGM). Composites Part B: Engineering 55:263-268

[8] Pradhan K, Chakraverty S (2013) Free vibration of Euler and Timoshenko functionally graded beams by Rayleigh–Ritz method. Composites Part B: Engineering 51:175-184

[9] Ansari R, Gholami R, Sahmani S (2013) Size-dependent vibration of functionally graded curved microbeams based on the modified strain gradient elasticity theory. Archive of Applied Mechanics 83 (10)

[10] Mashat DS, Carrera E, Zenkour AM, Al Khateeb SA, Filippi M (2014) Free vibration of FGM layered beams by various theories and finite elements. Composites Part B: Engineering 59:269-278

[11] Hadji L, Daouadji T, Tounsi A, Bedia E (2014) A higher order shear deformation theory for static and free vibration of FGM beam. Steel and Composite Structures 16 (5):507-519

[12] Sofiyev A (2015) On the vibration and stability of shear deformable FGM truncated conical shells subjected to an axial load. Composites Part B: Engineering 80:53-62

[13] Chen, Y., Jin, G., Zhang, C., Ye, T., & Xue, Y (2018) Thermal vibration of FGM beams with general boundary conditions using a higher-order shear deformation theory Composites Part B: Engineering 153:376-386.

[14] Zhang, K., Ge, M. H., Zhao, C., Deng, Z. C., & Xu, X. J (2019) Free vibration of nonlocal Timoshenko beams made of functionally graded materials by Symplectic method Composites Part B: Engineering 156:174-184.

[15] Wattanasakulpong N, Ungbhakorn V (2014) Linear and nonlinear vibration analysis of elastically restrained ends FGM beams with porosities. Aerospace Science and Technology 32 (1):111-120

[16] Ebrahimi F, Zia M (2015) Large amplitude nonlinear vibration analysis of functionally graded Timoshenko beams with porosities. Acta Astronautica 116:117-125

[17] Chen D, Yang J, Kitipornchai S (2016) Free and forced vibrations of shear deformable functionally graded porous beams. International Journal of Mechanical Sciences 108:14-22

[18] Shafiei N, Mousavi A, Ghadiri M (2016) On size-dependent nonlinear vibration of porous and imperfect functionally graded tapered microbeams. International Journal of Engineering Science 106:42-56

[19] Ebrahimi F, Ghasemi F, Salari E (2016) Investigating thermal effects on vibration behavior of temperature-dependent compositionally graded Euler beams with porosities. Meccanica 51 (1):223-249

[20] Taya, M., Almajid, A. A., Dunn, M., & Takahashi, H (2003) Design of bimorph piezo-composite actuators with functionally graded microstructure Sensors and Actuators A: Physical 107(3):248-260.

[21] She, G. L., Ren, Y. R., Yuan, F. G., & Xiao, W. S (2018) On vibrations of porous nanotubes International Journal of Engineering Science 125:23-35.

[22] Li Y, Shi Z (2009) Free vibration of a functionally graded piezoelectric beam via state-space based differential quadrature. Composite Structures 87 (3):257-264

[23] Armin A, Behjat B, Abbasi M, Eslami M (2010) Finite element analysis of functionally graded piezoelectric beams. Iran J Mech Eng (English) 11 (1):45-72

[24] Doroushi A, Eslami M, Komeili A (2011) Vibration analysis and transient response of an FGPM beam under thermo-electro-mechanical loads using higher-order shear deformation theory. Journal of Intelligent Material Systems and Structures 22 (3):231-243

[25] Ke L-L, Wang Y-S (2012) Thermoelectric-mechanical vibration of piezoelectric nanobeams based on the nonlocal theory. Smart Materials and Structures 21 (2):025018

[26] Barati MR, Zenkour AM (2016) Electro-thermoelastic vibration of plates made of porous functionally graded piezoelectric materials under various boundary conditions. Journal of Vibration and Control:1077546316672788

[27] Ebrahimi F, Salari E (2016) Thermal loading effects on electro-mechanical vibration behavior of piezoelectrically actuated inhomogeneous size-dependent Timoshenko nanobeams. Advances in Nano Research 4 (3):197-228

[28] Ebrahimi, F., & Barati, M. R (2018) Vibration analysis of piezoelectrically actuated curved nanosize FG beams via a nonlocal strain-electric field gradient theory Mechanics of Advanced Materials and Structures 25(4):350-359.

[29] Zhao, X., Iegaink, F. J. N., Zhu, W. D., & Li, Y. H (2019) Coupled thermo-electro-elastic forced vibrations of piezoelectric laminated beams by means

of Green's functions International Journal of Mechanical Sciences.

[30] Shen H-S (2005) Postbuckling of FGM plates with piezoelectric actuators under thermo-electro-mechanical loadings. International Journal of Solids and Structures 42 (23):6101-6121

[31] Ke L-L, Yang J, Kitipornchai S, Xiang Y (2009) Flexural vibration and elastic buckling of a cracked Timoshenko beam made of functionally graded materials. Mechanics of Advanced Materials and Structures 16 (6):488-502

[32] Cowper, G. R. (1966) The shear coefficient in Timoshenko's beam theory. *Journal of applied mechanics 33*(2):335-340.